Filsecker, F.; Alvarez, R.; Bernet, S., "Comparison of 4.5-kV Press-Pack IGBTs and IGCTs for Medium-Voltage Converters," *Industrial Electronics, IEEE Transactions on*, vol.60, no.2, pp.440-449, Feb. 2013

http://dx.doi.org/10.1109/TIE.2012.2187417

Comparison of 4.5 kV Press Pack IGBTs and IGCTs for Medium Voltage Converters

Felipe Filsecker, Rodrigo Alvarez, Steffen Bernet, *Member, IEEE*

***Abstract*—Recently developed Insulated Gate Bipolar Transistors (IGBT) press pack devices with a blocking voltage of 4.5 kV are being used in medium voltage converters as an alternative to Integrated Gate Commutated Thyristors (IGCT). This paper presents an overview of press pack packaging and both semiconductor technologies. A quantitative comparison of these devices is achieved through measurements for a 4.5 kV, 1.2 kA IGBT and a 4.5 kV, 4 kA IGCT. The laboratory test bench for the switching transient characterization at a dc-link voltage of 2.5 kV and currents up to 3 kA is described. Conduction, blocking and switching behavior for junction temperatures up to 125°C are investigated. The IGCT and the IGBT are tested using a $\mathrm{d}i/\mathrm{d}t$-limiting clamp circuit. Additionally, the IGBT is tested in hard switching mode.**

***Index Terms*—Power semiconductor devices, semiconductor losses, semiconductor measurements, IGBT, IGCT.**

I. INTRODUCTION

Medium voltage drives are essential for industry (e.g. oil and gas, chemistry, metals, marine, mining, etc.), traction and energy systems. They combine a high energy conversion efficiency and a highly dynamic control of the energy flow. Furthermore, medium voltage converters comply with the grid standards.

Power semiconductors have experienced a fast development towards higher blocking voltages and current ratings, more reliable packages and extended Safe Operating Areas (SOA) during the last years. They are an important technology driver for the further development of medium voltage converters. The application of medium voltage power semiconductor devices strongly depends on the converter voltage and current rating, as well as the application requirements. Today three different device types are applied in newly developed medium voltage converters: IGBTs, IGCTs and PCTs (Phase Controlled Thyristor). IGCTs and IGBTs can be separated into symmetrical, used in e.g current source and matrix converters, and asymmetrical, employed in voltage source converters (VSC) together with an antiparallel diode. Since VSCs are market standard today, only asymmetrical devices will be treated here. IGBTs clearly dominate at low power (Two Level- and Multi Level-VSCs: 2L-VSC, ML-VSC; converter power S_C = 300 kVA. . . 3 MVA). In contrast, load or grid commutated converters (e.g. LCIs or cycloconverters) with PCTs are applied in the majority of high power applications (e.g. $S_\mathrm{C} \geq 30$ MVA). In the medium power range (e.g. S_C = 3 MVA. . . 30 MVA) IGBTs and IGCTs compete with PCTs. [1]–[6]

The development trends of power semiconductors and topologies indicate that IGBT- and/or IGCT-based VSCs could replace medium power PCT-based converters (e.g. S_C = 10 MVA. . . 30 MVA) in the middle term, as current capacity and voltage ratings of ML-VSCs continue to increase. [7]–[9]

In the last years IGBTs have gained more and more importance in medium voltage converters. Lower conduction and switching losses, an extended Safe Operating Area, higher power and thermal power cycling capability and a broader junction temperature range are the reasons therefore, that IGBT modules have drastically increased their importance and market share. [10]–[14]

Press pack (PP) devices offer the potential of a higher power and thermal cycling capability. Furthermore, this package type does not explode in the majority of failure cases [15]. Press pack devices can be part of a redundant converter design, since the device stays short-circuited in failure case. In the case of high voltage applications, series connection is easily achieved by stacking the devices. Obviously, these characteristics are an advantage compared to modules. Nowadays, 4.5 kV IGCTs and IGBTs are available on the market as press packs. Both devices compete in Three Level-Neutral Point Clamped-Voltage Source Converters (3L-NPC VSCs) in a power range of $S_\mathrm{C} \approx$ 1 MVA. . . 30 MVA [4], [5]. In very high voltage applications, where many devices need to be connected in series, press-pack IGBTs devices are preferred over IGCTs, because of the lower gate driving power requirements.

This paper compares 4.5 kV IGCTs and recently introduced PP IGBTs. After a discussion of the characteristics of medium voltage IGCTs and IGBTs a test bench for the characterization of an IGCT and a PP IGBT is described. Both devices have very similar geometric dimensions and an identical diameter of 85 mm at the anode side or the collector side contact area. It should be noted that the PP IGBT is operated hard switched or with an adapted clamp circuit [16]–[18]. The operation with clamp circuit enables the investigation of the PP IGBT at identical conditions compared to the IGCT. Switching waveforms, trajectories and switching losses are the basis for a detailed comparison of both devices. The comparison considers the application point of view as well as the performance of the different semiconductor structures.

II. OVERVIEW OF MEDIUM VOLTAGE POWER SEMICONDUCTORS

Fig. 1 shows the nominal voltage and current ratings of commercially available MV IGBTs and asymmetrical IGCTs.

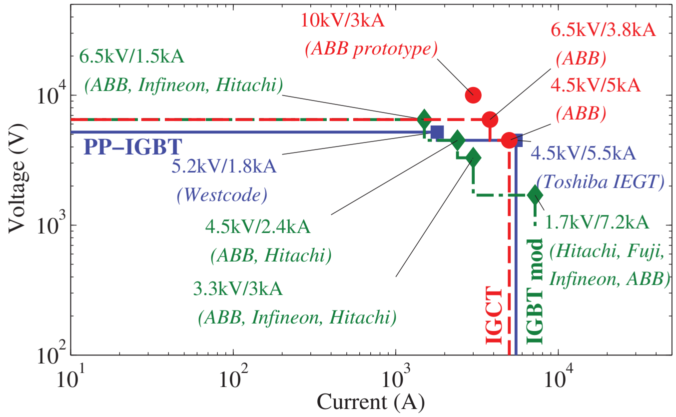

Fig. 1. Nominal ratings of power devices (IGCT: $V_{\mathrm{DRM}}/I_{\mathrm{TGQM}}$, IGBT: $V_{\mathrm{CES}}/I_{\mathrm{CM}}$) Status: Jan. 2012

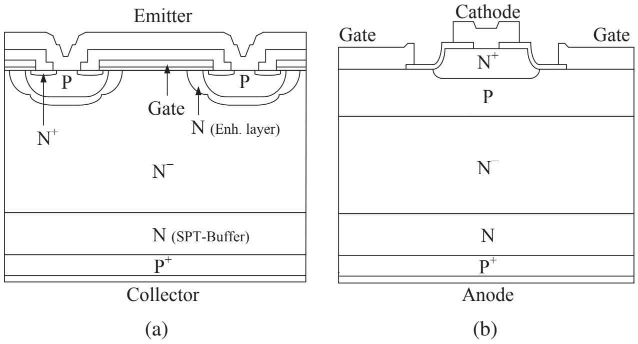

Fig. 2. Semiconductor structure: (a) IGBT SPT^+ [39] and (b) IGCT [21]

Structure and function of IGCTs and IGBTs have been extensively discussed in the literature (e.g. [1], [19]). Both IGBT modules and asymmetrical IGCTs feature a maximum device blocking voltage of 6.5 kV. New devices, such as 8 kV IGBTs and 10 kV IGCTs are still in research status [20]–[23].

The maximum turn-off current of IGCTs is given by the rated current I_{TGQM}. IGBTs current ratings include nominal current $I_{\mathrm{C,nom}}$ and maximum repetitive turn-off current I_{CM}. For a better comparison among device ratings, I_{TGQM} and I_{CM} are used in Fig. 1. Thus, a 125 mm 4.5 kV PP IGBT with $I_{\mathrm{C,nom}} = 2.4$ kA is able to turn off currents of $I_{\mathrm{C}} \leq 4.8$ kA. This current is slightly lower than that of the 91 mm 4.5 kV IGCT ($I_{\mathrm{TGQM}} = 5.5$ kA). A 125 mm 4.5 kV injection enhanced IGBT with $I_{\mathrm{C,nom}} = 2.1$ kA and capable of turning off a current of 5.5 kA has also been reported [24].

Even if it is considered that IGBTs are able to turn off twice the rated current, the power handling capability of IGBT modules is still substantially lower than that of IGCTs. However, PP IGBTs have a power handling capability which is close to that of 91 mm 4.5 kV IGCTs. Compared to IGCTs, PP IGBTs offer several advantages, like short circuit current limitation, short circuit turn-off capability, an adjustment of the switching behavior by the gate unit and a simple device parallel and series connection. Table I summarizes the characteristics of both technologies. The properties of the press pack and the module housing can be taken from Table II.

A. Press Pack IGBT With SPT^+ Technology

The basic structure of an IGBT with SPT^+ technology is depicted in Fig. 2a. This IGBT structure was developed to reduce the on-state losses, while keeping the switching losses low. This is achieved by the combination of a Soft-Punch-Through (SPT) buffer and an N-enhancement layer surrounding the P-well of the IGBT cell, improving the carrier concentration at the emitter side of the IGBT. With this approach, a wide SOA ($I_{\mathrm{C,max}} \geq I_{\mathrm{C,nom}}$) is obtained. [35]

In a PP IGBT, the single chips are connected in parallel. No solder or wire bond joints are required, avoiding possible failures due to power and thermal cycling [15], [33]. However, as a drawback, this configuration requires a passivation of every single die, loosing about half of the total silicon area. Furthermore, 20% of the circular press pack contact area is lost due to the squared chip form and the clearance between dies. PP IGBT would benefit from larger chip sizes, but the die manufacturing costs would increase considerably in that case. The die size for 4.5 kV PP IGBT used in this work is 204 mm^2 [36].

An IGBT gate unit has a simple basic design. In practical applications the gate drive is optimized to achieve minimum switching losses, a robust operation of the power semiconductors in the entire converter operating range, and a high reliability of power semiconductors and gate units. Well-engineered protection schemes are applied to handle short circuit currents or overvoltages. Usually the gate drive power is less than 5 W per IGBT. The placement of the gate unit is not complicated by strict requirements although a low inductive connection is always advantageous.

Even though IGBT technology has many years of development, the design is still evolving. New concepts, such as the BIGT, that combines IGBT and diode in one die, improving current and thermal distribution [37], or the Light Punch Through (LPT) structure [38] promise further improvements.

B. IGCT

The IGCT was introduced in 1990 as an enhancement to GTOs. The main difference was the low inductive connection between semiconductor and gate drive unit, which allowed a snubberless turn-off transient. Nevertheless, the IGCT turn-on transient still requires the use of a di/dt-limiting clamp.

Compared to IGBT modules or press packs consisting of small, discrete chips, the IGCT uses one large silicon wafer inside a press pack housing (e.g. 91 mm). The silicon wafer contains thousands of GCT-segments which are operated in parallel and sorted in concentric rings. The gate terminal is placed in the middle ring. The gate unit is connected by a very low inductive path (e.g. $L_\sigma = 5$ nH) to the wafer. It should be noted that the complete anode current flows to the gate unit for a few microseconds during turn-off transients, thus

TABLE I
PROPERTIES OF IGCT AND IGBT

Characteristics	IGCT [25]–[27]	IGBT [25]–[27]
Clamp circuit	Limits $\mathrm{d}i/\mathrm{d}t$ and short circuit current	Not required
On-state voltage	Low	High
Turn-on losses	Low (due to clamp circuit)	High (hard switching)
Turn-off losses	Higher than a comparable IGBT	Lower than a comparable IGCT
Switching behavior	Determined by device structure, doping and clamp circuit	Adjustable by the gate unit
Clamp Losses	Yes	No (hard switching)
Gate unit power	Medium (typically 100 W/device)	Low (typically 5 W/device)
Reliability	About 100 FIT (field data)	About 100 FIT (field data)
Short circuit current	Not limited [28]	Limited (operation in the active region)
	Discharge of dc-link capacitors	Active short circuit current turn-off [29]
Maximum surge current	High	Low
Overvoltage limitation	By clamp circuit	Low stray inductance & suitable gate driving
Parallel connection	Complex, bulky external balancing network [30]	Simple, low parameter deviation and adjustment by gate unit
Series connection	Complex, bulky external balancing network [31]	Simple, gate unit control ($\mathrm{d}v/\mathrm{d}t$, active clamping) + static balancing resistor [32]

TABLE II
PROPERTIES OF MODULE AND PRESS PACK HOUSING

Feature	Module [25], [26], [33]	Press Pack [15], [25], [26]
Explosion free [34]	No, possible explosion at "double failure"	Mostly (exception: failure at edge passivation)
Cooling	Simple, cooling by isolated heat sink	More expensive cooling (deionized water)
Mounting	Simple, mounting on isolated heat sink	More expensive mounting in stack
Power and thermal cycling capability	Low-medium: thermo-mechanical stress of bond wires and solder between plate and DCB	High, no bond wires and solder connections
Redundancy	No, undefined state after failure	Possibility of redundant converter design, due to the safe short circuit failure mode in most failure cases

Fig. 3. IGCT 5SHY 35L4503 (left) and IGBT T1200EB45E with gate unit (right)

determining the size and power of the gate unit [21]. Gate unit power consumption is in the range of 50 to 150 W, depending on the switching frequency and operating conditions. This is one of the drawbacks of this technology, when compared to IGBT gate driving.

The active silicon area in the IGCT differs from the total area of the wafer, because it contains only the area encapsulated by the thyristor segments, including the gate area between the neighboring segments, but not including the gate ring, the test structures in the center and the edge terminations.

Lately, IGCT and gate unit design have been improved to increase the maximum turn-off current [40]. The combined innovations are referred as High-Power Technology (HPT). Compared to the conventional IGCT, the HPT offers a 40% increased current rating. HPT IGCTs are available for blocking voltages of 4.5 and 6.5 kV. Last improvements in IGCT technology also include the developement of gate units placed inside the press pack and dual GCTs, which include two devices in one wafer [41], [42]. In this paper, a conventional IGCT device

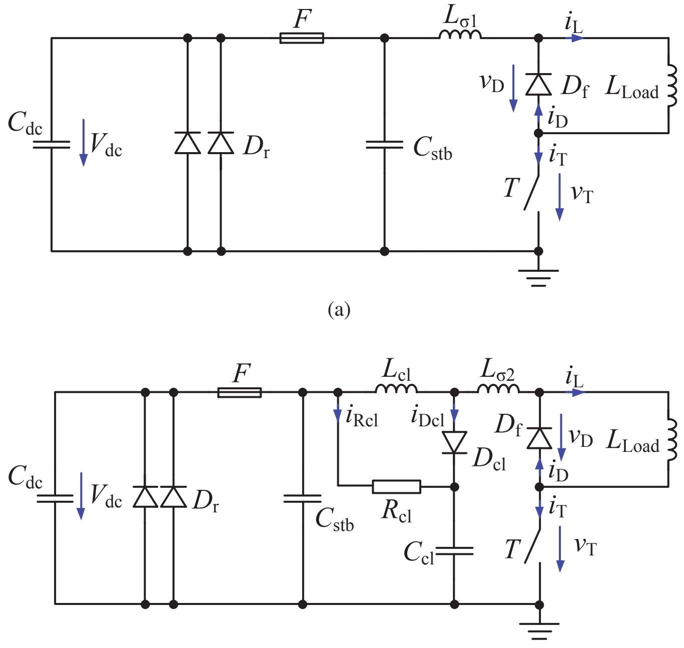

(a)

(b)

Fig. 4. Test circuit configuration for (a) hard switching (T: IGBT) and (b) clamp operation (T: IGBT or IGCT)

was tested.

III. SEMICONDUCTOR DATA AND TEST BENCH

For the comparison, 4.5 kV IGCTs and PP IGBTs have been investigated. Both devices have a diameter of 85 mm at the anode side and the collector side contact area respectively. The IGCT uses a wafer with a diameter of 91 mm. In contrast, the PP IGBT contains 21 dies with a total silicon area of 204 mm^2 per die.

The PP IGBTs are operated hard switched and also in the same clamp configuration as the IGCT. The clamp circuit is required for IGCTs to limit the di/dt of the turning-off diode and the turning-on IGCT. In the case of IGBTs, the clamp has the same effect, which translates into a stress reduction for the IGBT during the turn-on transient.

Further relevant semiconductor data can be found in Table III. It is important to note that the maximum turn-off current of the IGCT ($I_{\mathrm{TGQM}} = 4\,\mathrm{kA}$) is 67% higher than that of the IGBT ($I_{\mathrm{CM}} = 2.4\,\mathrm{kA}$). The active silicon area of the IGCT is almost twice as large as that of the PP IGBT. The configuration of the test circuits is shown in Fig. 4. The design of the clamp can be taken from Table IV. Fig. 4a shows the circuit configuration for the hard switching IGBT. In contrast, the circuit with clamp configuration for the IGCT and the IGBT can be taken from Fig. 4b.

The test circuit corresponds to a buck converter, which allows the investigation of the switching behavior of the active switch (e.g. IGBT, IGCT) and the freewheeling diode, by the use of a double-pulse switching pattern [43]. Hard-switching devices demand a low stray inductance in the commutation circuit ($L_{\sigma 1}$ in Fig. 4a) to avoid large overvoltages at turn-off transients. The arrangement of a low inductive capacitor C_{stb} (220 µF) close to the stack enables a stray inductance of $L_\sigma \approx 130\,\mathrm{nH}$ in the commutation path.

A robust mechanical design was accomplished using 2 mm-thick copper plates connecting the dc-link capacitor C_{dc}, the stabilizing capacitor C_{stb} and the stack. Thus, the mechanical construction of the test bench is able to withstand short circuit currents of about 200 kA in case of a device failure. The two diodes D_{r} and the fuse F are important components of the protection concept. The fuse avoids the complete discharge of the dc-link capacitors through the stack, and the D_{r} diodes limit possible negative voltages across the dc-link capacitor, preventing an oscillation of the short circuit current.

The junction temperatures of the devices are adjusted by two ring heaters mounted in the stack, controlling the case temperatures of the active switch and the diode. The dc-link capacitor is charged by a high voltage power supply before the measurements are carried out. A partially automated measurement system was used. The values of V_{dc} and I_{L} are set through a LabVIEW graphical user interface in a computer connected to the test bench by fiber-optic cable. The results are captured by two 8 bit four-channel digital oscilloscopes (Tektronix TDS714L), capable of working at 500 MS/s sample rate. The storage and analysis of the data is carried out on a PC.

Considering a commutation voltage of $V_{\mathrm{dc}} = 2.5\,\mathrm{kV}$, the clamp circuit (see Fig. 4b) was designed to limit the di/dt during turn-on transients to a value of 450 A/µs using an inductor of $L_{\mathrm{cl}} = 5.6\,\mu\mathrm{H}$. Clamp capacitor ($C_{\mathrm{cl}} = 10\,\mu\mathrm{F}$) and resistor ($R_{\mathrm{cl}} = 0.5\,\Omega$) have been chosen to demagnetize the clamp inductor within 27 µs after the IGCT/IGBT turn-off transients. The peak voltage due to the clamp inductor demagnetization reaches 4500 V at a current of 6000 A ($5I_{\mathrm{C,nom}}$ of the IGBT).

The experimental setup is shown in Fig. 5. The measurements for both IGCT and IGBT tests were carried out at a dc-link voltage V_{dc} of 2500 V. The IGCT was switched at currents ranging from 200 to 3000 A, whereas the IGBT at currents from 100 to 1500 A. For driving the IGBT a Westcode gate unit model C0030BG400, with $R_{\mathrm{G,on}} = 3.3\,\Omega$, $R_{\mathrm{G,off}} = 2.2\,\Omega$, $V_{\mathrm{G,on/off}} = \pm 15\,\mathrm{V}$ and $P_{\mathrm{o}} = 12\,\mathrm{W}$ was used.

IV. COMPARISON OF IGCTS AND PP IGBTS

A. Conduction and Blocking Characteristics

Conduction and blocking characteristics are shown in Fig. 6 and Fig. 7 for IGBT and IGCT. Both characteristics have been determined experimentally using the same test circuit and comparable conditions.

Regarding the on-state characteristics, the higher on-state voltage of the IGBT is significant. To compare devices with different structures and manufacturing technologies from a physical point of view, the current density is a decisive parameter. Fig. 6 also shows the on-state voltage as a function of the device current density. Considering a junction temperature of $T_{\mathrm{j}} = 125\,^{\circ}\mathrm{C}$, the IGBT on-state voltages are about 130%

TABLE III
SELECTED SEMICONDUCTOR DATA

Device	IGCT	IGBT	Freewheeling diode D_f IGCT test	Freewheeling diode D_f IGBT test
Manufacturer	ABB	Westcode	Infineon	Infineon
Model	5SHY 35L4503	T1200EB45E	D 1331SH	D 1031SH
Diameter (contact surface)	85 mm	85 mm	85 mm	63 mm
Si-area	$6504\,\mathrm{mm}^2$	$4284\,\mathrm{mm}^2$	$5809\,\mathrm{mm}^2$	$3097\,\mathrm{mm}^2$
Active Si-area A_aSi	$4290\,\mathrm{mm}^2$	$2142\,\mathrm{mm}^2$	$3526\,\mathrm{mm}^2$	$2463\,\mathrm{mm}^2$
R_thJH (double-sided cooling)	18 K/kW	8 K/kW	11.05 K/kW	14.1 K/kW
Forward blocking voltage	4500 V	4500 V	4500 V	4500 V
$V_\mathrm{DC\text{-}link}$	2800 V	2800 V	–	–
I_TGQM	4000 A	–	–	–
$I_\mathrm{C,nom}$ / I_CM	–	1200 A/2400 A	–	–
I_FRMSM	–	–	2730 A	2300 A
I_FAVM	–	–	1740 A	1470 A
I_RM	–	–	1500 A	1500 A
$J(I_\mathrm{TGQM})$, $J(I_\mathrm{CM})$	$93.2\,\mathrm{A/cm}^2$	$112\,\mathrm{A/cm}^2$	–	–

TABLE IV
DATA OF CIRCUIT AND CLAMP CONFIGURATION

Test bench		Clamp circuit	
C_dc	4.5 mF	C_cl	10 µF
C_stb	220 µF	R_cl	0.5 Ω
L_Load	1 mH	L_cl	5.6 µH
V_dc	2.5 kV		
$L_{\sigma 1}$	130 nH	$L_{\sigma 2}$	130 nH

TABLE V
VOLTAGE AND CURRENT SLOPES†

	IGCT (clamp)	IGBT (clamp)	IGBT (hard)
di/dt turn-on (kA/µs)	0.49	0.52	4.03
di/dt turn-off (kA/µs)	–1.22	–1.32	–1.47
dv/dt turn-on (kV/µs)	–5.09	–3.46	–3.12
dv/dt turn-off (kV/µs)	1.97	2.40	2.59

† V_dc = 2.5 kV, I_L = 1.5 kA, L_σ = 130 nH, T_j = 125 °C, values calculated as in [16], [17].

higher than those of the IGCT (ΔV_on = 1.3…2.5 V). Obviously, this is an important disadvantage for low switching frequency applications where the on-state losses dominate.

IGCTs and IGBTs have similar leakage current characteristics, as seen in Fig. 7. Among the differences, IGBT leakage current stays under 17 µA for 25 °C. IGCT current, on the other hand, grows exponentially, going from nearly zero at 2.5 kV up to 8 mA at 4.5 kV. At a junction temperature of T_j = 125 °C the leakage currents of IGCTs and PP IGBTs are nearly identical in the relevant blocking voltage range ($2\,\mathrm{kV} \leq V_\mathrm{dc} \leq 4.5\,\mathrm{kV}$).

B. Switching Behavior

Figs. 8 to 10 show waveforms, VI-plane traces and instantaneous power at a load current of $I_\mathrm{L} = 1.5\,\mathrm{kA}$ for the three different switch configurations. Voltage and current slopes during the commutations are summarized in Table V.

During the turn-off transient (Fig. 8) the stray inductance $L_{\sigma 2}$ is the reason for the first overvoltage spike (during the collector-current fall). The second overvoltage, including its maximum at about 10 µs after the begin of the turn-off transient, is caused by the demagnetization of L_cl. As a result, the IGBT turn-off losses with clamp are ≈ 8% higher compared to hard switching. The lower dv_T/dt and the longer tail current of the IGCT generate higher turn-off losses compared to the IGBT.

The IGCT turn-off transient exhibits a slightly lower dv/dt and di/dt compared to the IGBT with clamp circuit. Thus, peak power and turn-off losses are slightly higher in the IGCT (≈ +10%). Even though the peak power is similar in both devices, there is an important difference in the peak power density. The stress experimented by the IGCT with $8.8\,\mathrm{kW/cm}^2$ is around 50% lower than the one in the IGBT.

During the turn-on transient (Fig. 9) the switching losses and the corresponding device stress are substantially reduced by the clamp circuit. The turn-on behavior of IGCT and IGBT with clamp is very similar. The device voltage falls immediately after the delay time. In the case of the hard switching IGBT, the device voltage falls only when the freewheeling diode takes over reverse blocking voltage. The collector current increases while the device blocks a substantial amount of the commutation voltage, which generates high losses.

Also the turn-off behavior of the freewheeling diode is influenced by the circuit configuration. Comparing IGBT and IGCT with clamp, the diode waveforms are very similar. The slightly higher peak reverse recovery current of the IGCT freewheeling diode D 1331SH causes a small increase of the instantaneous power maximum value. In the case of the hard switching IGBT, the peak reverse recovery current and the

(a)

(b)

(c)

Fig. 5. Experimental setup: (a) di/dt-clamp circuit, (b) IGCT stack, (c) IGBT stack for hard switching

maximum value of the instantaneous power are increased by 151% and 68% respectively, compared to the IGBT with clamp.

Noteworthy is that in Figs. 8 to 10 the IGCT was switched at 40% of I_{TGQM} and the IGBT at 125% of $I_{\text{C,nom}}$, which corresponds to 63% of $2I_{\text{C,nom}}$. These values correspond to current densities of 34 A/cm^2 for the IGCT and 68 A/cm^2 for the IGBT.

The total semiconductor switching losses are given by

$$E_{\text{SC}} = E_{\text{on,T}} + E_{\text{off,T}} + E_{\text{off,D}} \tag{1}$$

with

$E_{\text{on,T}}$: IGBT / IGCT T turn-on losses
$E_{\text{off,T}}$: IGBT / IGCT T turn-off losses
$E_{\text{off,D}}$: freewheeling diode D_{f} turn-off losses

These losses only reflect switching losses in the semiconductors and do not include the clamp circuit losses. Total switching losses (semiconductors + clamp circuit) for IGBTs with and without clamp circuit do not vary considerably [17].

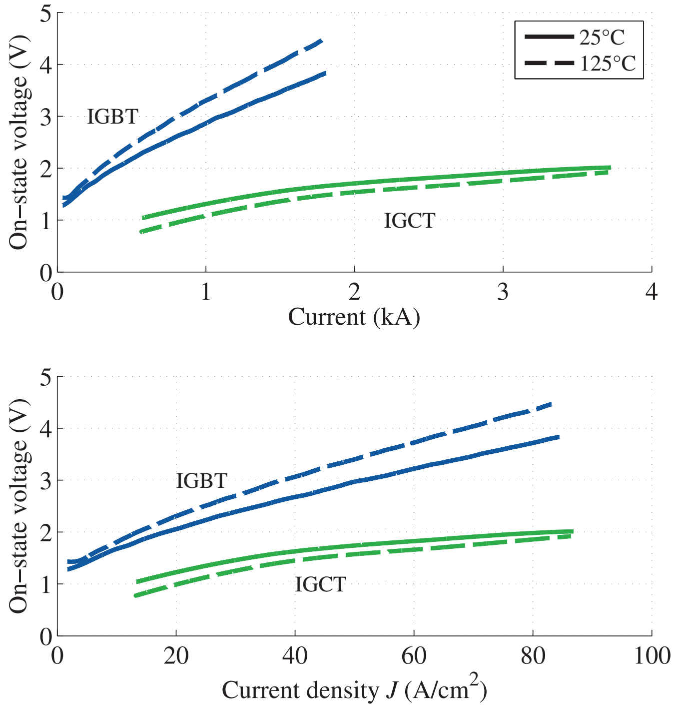

Fig. 6. On-state characteristics

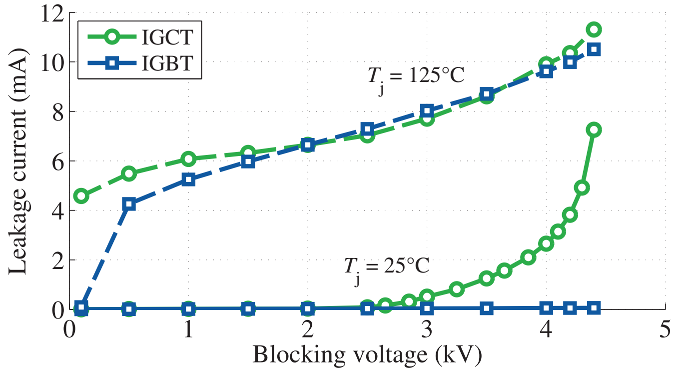

Fig. 7. Leakage currents as a function of blocking voltage

Figure 11 shows the device switching losses as a function of the load current. This representation is important for the application of the semiconductors in a converter from a practical point of view. As expected, the IGBT turn-on losses at hard switching are considerably higher compared to the clamp operation of IGBT and IGCT. The IGBT with clamp realizes slightly lower turn-on losses than the IGCT. The IGBT turn-off losses with or without clamp are very similar. They are reduced by about 15% and 22% compared to the IGCT at I_{L} = 1500 A. The diode turn-off losses are comparable for all three switch configurations. Considering the total switching losses, the IGBT causes 14% lower losses with clamp and 29% higher losses at hard switching compared to the IGCT at I_{L} = 1500 A.

The switching losses as a function of the device current density $J = I_{\text{L}}/A_{\text{aSi}}$ are given in Fig. 12. Furthermore, Fig. 11 depicts the current densities at selected load current values. Figure 12 shows that the IGBT with clamp realizes lower turn-

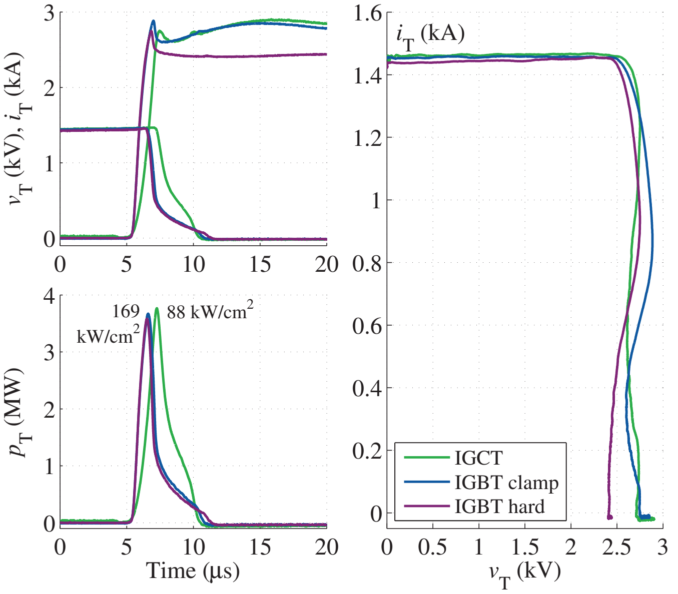

Fig. 8. IGBT/IGCT turn-off behavior: Voltage v_T and current i_T waveforms, instantaneous power p_T and VI-plane traces (V_dc = 2.5 kV, I_L = 1.5 kA, L_σ = 130 nH, T_j = 125 °C)

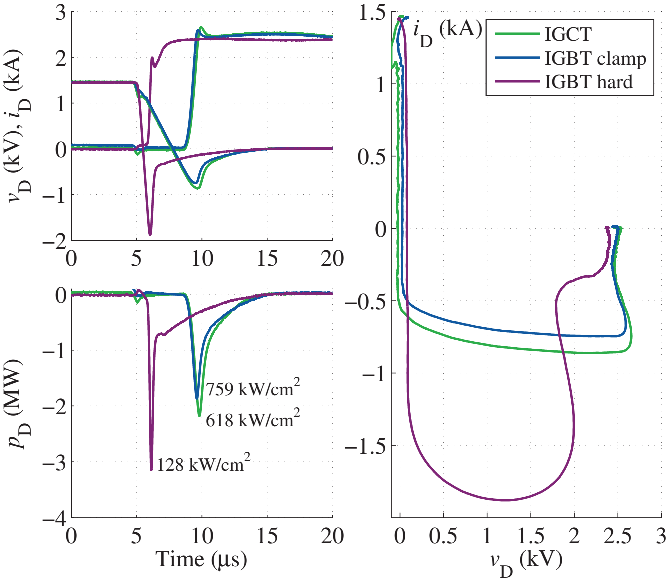

Fig. 10. Diode turn-off behavior: Voltage v_D and current i_D waveforms, instantaneous power p_D and VI-plane traces (V_dc = 2.5 kV, I_L = 1.5 kA, L_σ = 130 nH, T_j = 125 °C)

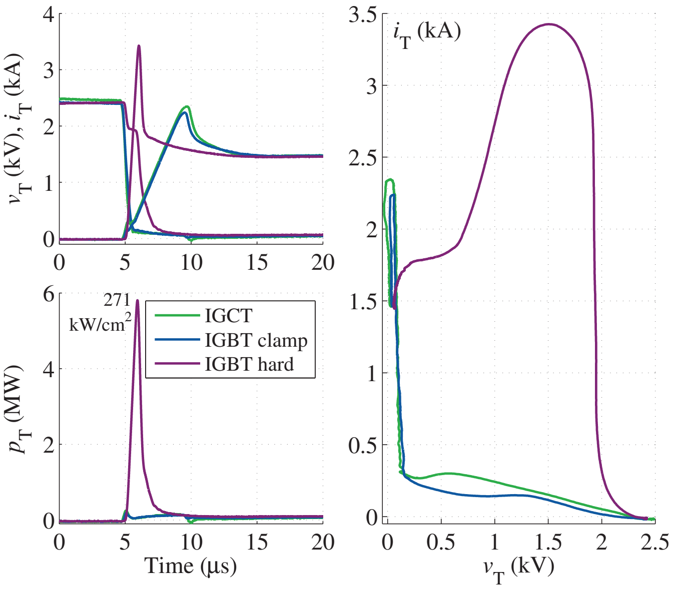

Fig. 9. IGBT/IGCT turn-on behavior: Voltage v_T and current i_T waveforms, instantaneous power p_T and VI-plane traces (V_dc = 2.5 kV, I_L = 1.5 kA, L_σ = 130 nH, T_j = 125 °C)

on losses than the IGCT. The hard switching IGBT causes substantially increased turn-on losses. The turn-off losses of the IGBT with or without clamp are more than 50% lower than the IGCT turn-off losses. When considering both turn-on and turn-off losses, the IGBT with clamp has clearly less losses. These are about 40% lower than the hard switching IGBT losses and 54% lower than the IGCT losses.

The diode turn-off losses of both IGBT configurations are lower than that of the IGCT freewheeling diode, e.g. by 19% (IGBT with clamp) and 10% (hard switching IGBT) at $J = 60\,\mathrm{A/cm^2}$.

C. Comparison from an application point of view

From an application point of view, the IGCT has the advantage of a substantially increased maximum turn-off current ($I_\mathrm{TGQM} = 4000\,\mathrm{A}$ (IGCT), $I_\mathrm{CM} = 2400\,\mathrm{A}$ (IGBT)) at similar geometrical dimensions. Furthermore, the on-state voltages of the IGCTs are substantially lower at identical device currents (e.g. $V_\mathrm{on,IGCT} = 1.4\,\mathrm{V}$, $V_\mathrm{on,IGBT} = 4.0\,\mathrm{V}$ at $I_\mathrm{L} = 1500\,\mathrm{A}$, T_j = 125 °C).

The IGBT with clamp shows a better switching behavior than the IGCT (e.g. a reduction of turn-on losses by 51% and of turn-off losses by 15% at $I_\mathrm{L} = 1500\,\mathrm{A}$). Compared to the hard switching IGBT, the clamp configuration enables a drastic reduction of the IGBT turn-on losses (e.g. by 95% at $I_\mathrm{L} = 1500\,\mathrm{A}$). Although the maximum instantaneous power of the diode is maximal at hard switching, the diode turn-off losses of all three switch configurations are similar.

It is obvious that for similar geometrical dimensions, the PP IGBT suffers from the limited IGBT die size, the large passivation area and the round press pack housing. If IGCT and IGBT at comparable active silicon areas are considered, a 125 mm PP IGBT must be compared with the analyzed 91 mm IGCT. In this case, the characteristics of the device structures are decisive.

D. Comparison of IGBT and IGCT at die level

It is interesting to note that the current density of the IGBT at the maximum device turn-off current is 20% higher than that

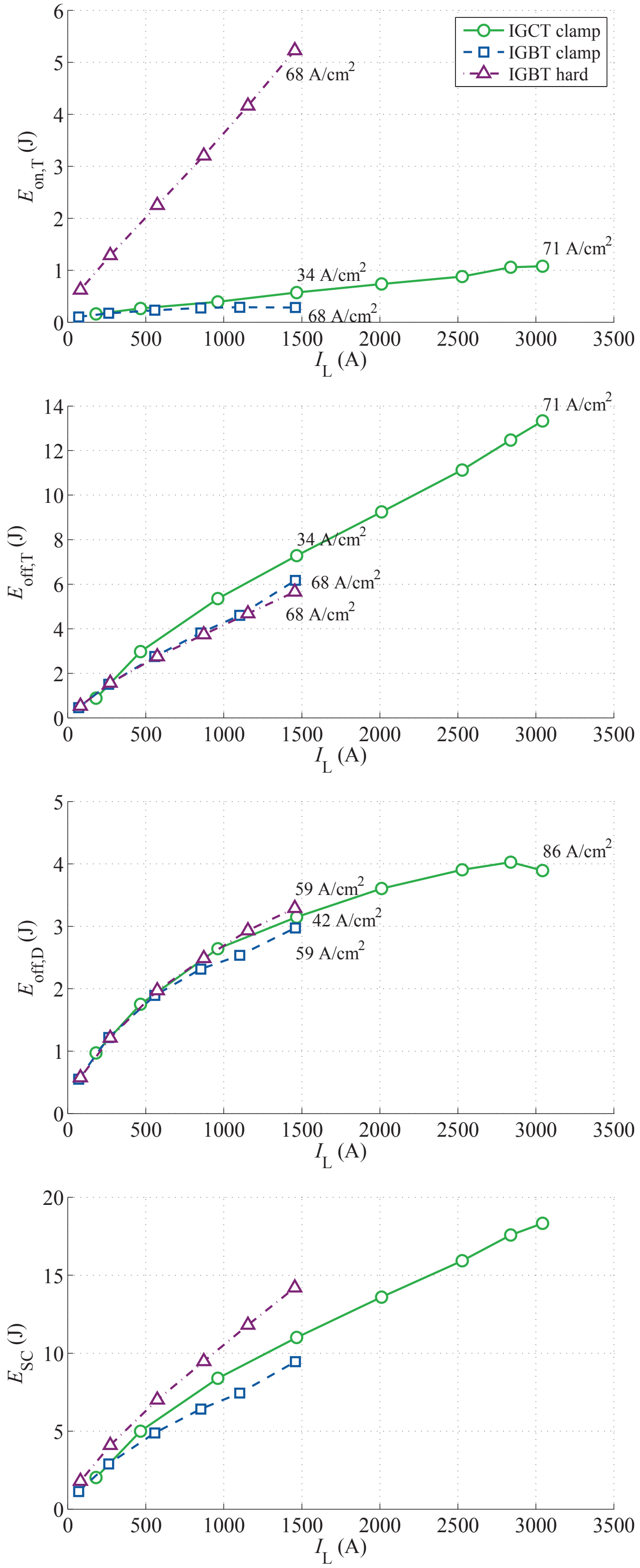

Fig. 11. Losses against load current I_{L}: total semiconductor switching losses E_{SC}, active switch turn-on losses $E_{\mathrm{on,T}}$, active switch turn-off losses $E_{\mathrm{off,T}}$ and diode turn-off losses $E_{\mathrm{off,D}}$ (V_{dc} = 2500 V, L_σ = 130 nH, T_{j} = 125 °C)

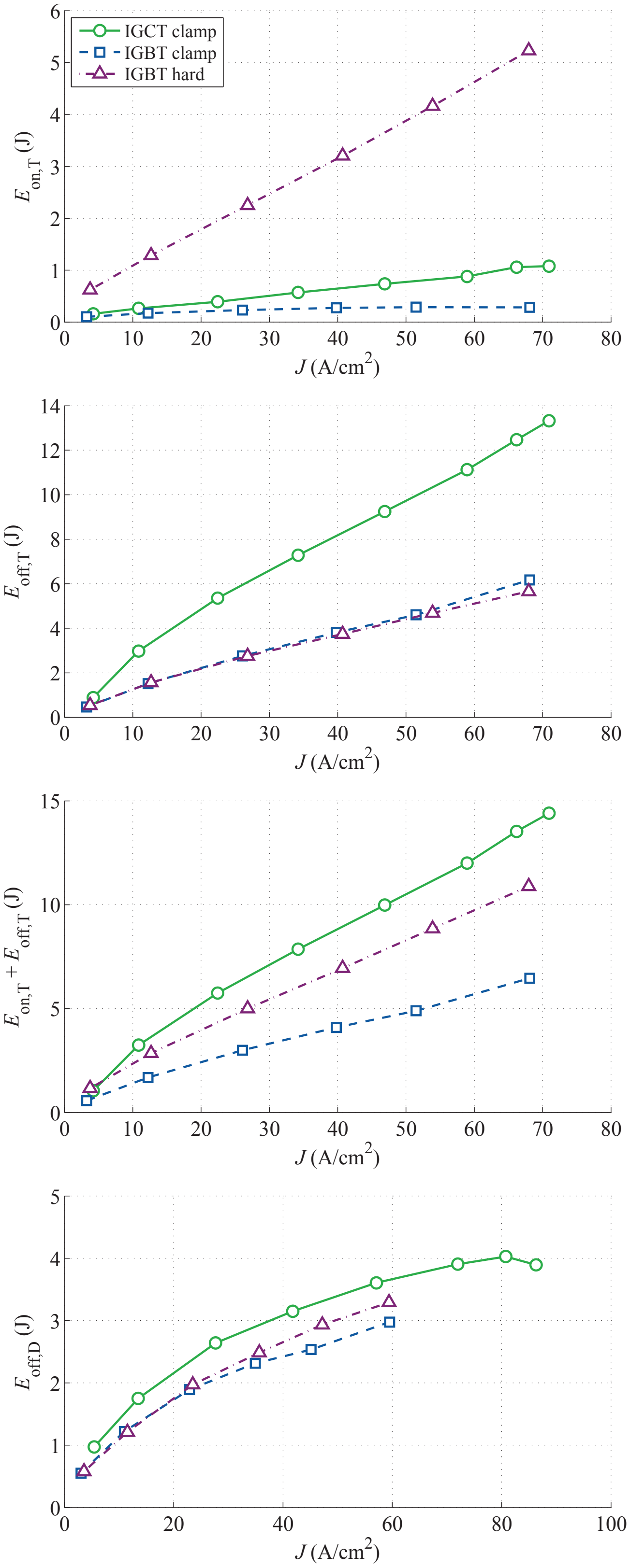

Fig. 12. Losses against load current density $J = I_{\mathrm{L}}/A_{\mathrm{aSi}}$: active switch turn-on losses $E_{\mathrm{on,T}}$, active switch turn-off losses $E_{\mathrm{off,T}}$, active switch turn-on and turn-off losses $E_{\mathrm{on,T}}$ + $E_{\mathrm{off,T}}$ and diode turn-off losses $E_{\mathrm{off,D}}$ (V_{dc} = 2500 V, L_σ = 130 nH, T_{j} = 125 °C)

of the IGCT (IGBT: J = 112 A/cm^2 at I_{CM} = 2400 A, IGCT: J = 93.2 A/cm^2 at I_{TGQM} = 4000 A). If the IGBT is operated in the same circuit configuration as the IGCT, the switching losses are substantially lower in the entire current density range. Exemplarily, the IGBT switching losses are reduced by about 23% (hard switching) and 54% (clamp operation) at T_{j} = 125 °C. Since the IGBT has a higher on-state voltage, the lowest losses are generated by the IGCT at low and by the IGBT at medium to high switching frequencies.

V. CONCLUSIONS

In this paper, 85 mm 4.5 kV IGCTs and PP IGBTs are compared. Both semiconductors have very similar geometric dimensions. However, the limited maximum die size of IGBTs, the corresponding large passivation area and the packaging of the IGBT dies in a round press pack housing are the reasons therefore, that the active silicon area of the PP IGBT is only 50% compared to the IGCT. The PP IGBTs are operated hard switched and in a clamp configuration which is identical to that of the IGCT.

The operation of IGBTs with clamp circuit is an effective method to decrease the device switching losses. Thus, an increase of the converter power and/or the switching frequency can be achieved. As a drawback, additional expenses for the clamp circuit and additional clamp losses have to be considered [17]. Nevertheless, it is expected that IGBTs with clamp operation will increasingly be applied in medium voltage, high power applications.

IGCTs enable a higher switch utilization than PP IGBTs with clamp, due to the higher turn-off current capability for equal disc area, and the lower on-state voltages despite the slightly higher switching losses. Compared to hard switching IGBTs, the switch utilization of the IGCT is further increased due to the reduced switching losses. [1], [2]

Comparing IGCTs and PP IGBTs at similar current densities and active silicon areas, the investigations show a higher turn-off current capability, higher on-state voltages and lower switching losses for the IGBT. While the on-state voltages of the IGBT are increased by 0.8. . . 2.5 V, its switching losses are reduced by about 23% at hard switching and 54% at clamp operation.

Taking the further advantages of the IGBT structure like the short circuit turn-off capability, the adjustment of the switching speed by the gate unit, the low gate drive power, the possible avoidance of clamp components as well as the simple series and parallel connection into account, the IGBT structure is superior in the majority of characteristics and applications. Considering the high innovation potential of IGBTs and the high degree of maturity of IGCTs, a further increase of the importance of IGBTs is expected for the future.

REFERENCES

[1] J. Vobecky, "Design and technology of high-power silicon devices," in *Mixed Design of Integrated Circuits and Systems (MIXDES), 2011 Proceedings of the 18th International Conference*, June 2011, pp. 17–22.

[2] A. Chattopadhyay, "Alternating current drives in the steel industry," *Industrial Electronics Magazine, IEEE*, vol. 4, no. 4, pp. 30–42, Dec. 2010.

[3] S. Bernet, R. Teichmann, A. Zuckerberger, and P. Steimer, "Comparison of high-power IGBTs and hard-driven GTOs for high-power inverters," *IEEE Trans. Ind. Appl.*, vol. 35, no. 2, pp. 487–495, Mar./Apr. 1999.

[4] J. Rodriguez, S. Bernet, P. Steimer, and I. Lizama, "A survey on neutral-point-clamped inverters," *IEEE Trans. Ind. Electron.*, vol. 57, no. 7, pp. 2219–2230, July 2010.

[5] S. Kouro, M. Malinowski, K. Gopakumar, J. Pou, L. Franquelo, B. Wu, J. Rodriguez, M. Perez, and J. Leon, "Recent advances and industrial applications of multilevel converters," *IEEE Trans. Ind. Electron.*, vol. 57, no. 8, pp. 2553–2580, Aug. 2010.

[6] J. Rodriguez, S. Bernet, B. Wu, J. Pontt, and S. Kouro, "Multilevel voltage-source-converter topologies for industrial medium-voltage drives," *IEEE Trans. Ind. Electron.*, vol. 54, no. 6, pp. 2930–2945, Dec. 2007.

[7] M. Hiller, R. Sommer, and M. Beuermann, "Converter topologies and power semiconductors for industrial medium voltage converters," in *Industry Applications Society Annual Meeting, 2008. IAS '08. IEEE*, Edmonton, Alberta, Canada, Oct. 2008, pp. 1–8.

[8] C. Wang, C. Li, Y. Li, C. Zhu, and Z. Lan, "Large power three-level voltage source inverter with IGCTs and the experiment," in *Energy Conversion Congress and Exposition (ECCE), 2010 IEEE*, Sept. 2010, pp. 2087–2090.

[9] T. Bruckner and R. Jakob, "New medium-voltage inverter design with very high power density," in *Power Electronics Specialists Conference, 2008. PESC 2008. IEEE*, June 2008, pp. 2962–2967.

[10] M. Liserre, R. Cardenas, M. Molinas, and J. Rodriguez, "Overview of multi-MW wind turbines and wind parks," *IEEE Trans. Ind. Electron.*, vol. 58, no. 4, pp. 1081–1095, Apr. 2011.

[11] O. Senturk, L. Helle, S. Munk-Nielsen, P. Rodriguez, and R. Teodorescu, "Converter structure-based power loss and static thermal modeling of the press-pack IGBT-based three-level ANPC and HB VSCs applied to multi-MW wind turbines," in *Energy Conversion Congress and Exposition (ECCE), 2010 IEEE*, Sept. 2010, pp. 2778–2785.

[12] J. Sayago, T. Bruckner, and S. Bernet, "How to select the system voltage of MV drives: A comparison of semiconductor expenses," *IEEE Trans. Ind. Electron.*, vol. 55, no. 9, pp. 3381–3390, Sept. 2008.

[13] D. Krug, S. Bernet, S. Fazel, K. Jalili, and M. Malinowski, "Comparison of 2.3-kV medium-voltage multilevel converters for industrial medium-voltage drives," *IEEE Trans. Ind. Electron.*, vol. 54, no. 6, pp. 2979–2992, Dec. 2007.

[14] J. Carrasco, L. Franquelo, J. Bialasiewicz, E. Galvan, R. Guisado, M. Prats, J. Leon, and N. Moreno-Alfonso, "Power-electronic systems for the grid integration of renewable energy sources: A survey," *IEEE Trans. Ind. Electron.*, vol. 53, no. 4, pp. 1002–1016, June 2006.

[15] F. Wakeman and G. Lockwood, "Electromechanical evaluation of a bondless pressure contact IGBT," *IEE Proceedings Circuits, Devices and Systems*, vol. 148, no. 2, pp. 89–93, Apr. 2001.

[16] R. Alvarez, F. Filsecker, and S. Bernet, "Characterization of a new 4.5 kV press pack SPT+ IGBT for medium voltage converters," in *Energy Conversion Congress and Exposition (ECCE), 2009 IEEE*, San Jose, USA, Sept. 2009, pp. 3954–3962.

[17] R. Alvarez, S. Bernet, L. Lindenmueller, and F. Filsecker, "Characterization of a new 4.5 kV press pack SPT+ IGBT in voltage source converters with clamp circuit," in *Industrial Technology, 2010. ICIT 2010. IEEE International Conference on*, Viña del Mar, Chile, March 2010.

[18] F. Kieferndorf, M. Basler, L. Serpa, J. Henning, A. Coccia, and G. Scheuer, "A new medium voltage drive system based on ANPC-5L technology," in *Industrial Technology, 2010. ICIT 2010. IEEE International Conference on*, Viña del Mar, Chile, March 2010.

[19] M. Rahimo and S. Klaka, "High voltage semiconductor technologies," in *Power Electronics and Applications, 2009. EPE '09. 13th European Conference on*, Barcelona, Spain, Sept. 2009, pp. 1–10.

[20] S. Bernet, E. Carroll, P. Streit, O. Apeldoorn, P. Steimer, and S. Tschirley, "10 kV IGCTs," *Industry Applications Magazine, IEEE*, vol. 11, no. 2, pp. 53–61, Mar./Apr. 2005.

[21] I. Nistor, T. Wikstrom, and M. Scheinert, "IGCTs: High-Power Technology for power electronics applications," in *Semiconductor Conference, 2009. CAS 2009. International*, vol. 1, Oct. 2009, pp. 65–73.

[22] M. Rahimo, A. Kopta, S. Eicher, N. Kaminski, F. Bauer, U. Schlapbach, and S. Linder, "Extending the boundary limits of high voltage IGBTs and

diodes to above 8 kV," in *Power Semiconductor Devices and ICs, 2002. Proceedings of the 14th International Symposium on*, 2002, pp. 41–44.

[23] M. Rahimo, P. Streit, A. Kopta, U. Schlapbach, S. Eicher, and S. Linder, "The status of IGBTs and IGCTs rated over 8kV," *24th PCIM Europe, Nürnberg, Germany*, 2003.

[24] K. Ichikawa, M. Tsukakoshi, and R. Nakajima, "Higher efficiency three-level inverter employing IEGTs," in *Applied Power Electronics Conference and Exposition, 2004. APEC'04. Nineteenth Annual IEEE*, vol. 3, 2004.

[25] S. Bernet, "Recent developments of high power converters for industry and traction applications," *IEEE Trans. on Power Electron.*, vol. 15, no. 6, pp. 1102–1117, Nov. 2000.

[26] S. Bernet, "State of the art and developments of medium voltage converters – An overview," *Przegląd Elektrotechniczny*, vol. 82, no. 5, pp. 1–10, 2006.

[27] T. Schuetze, H. Berg, and O. Schilling, "The new 6.5 kV IGBT module: a reliable device for medium voltage applications," in *Proceedings of PCIM Europe 2001*, 2001.

[28] A. Rocha, G. Frana, M. dos Santos, H. de Paula, and B. Cardoso Filho, "Improving the performance of protection schemes in three level IGCT-based neutral point clamped converters," in *Energy Conversion Congress and Exposition (ECCE), 2010 IEEE*, Sept. 2010, pp. 2326–2332.

[29] V. John, B.-S. Suh, and T. Lipo, "Fast-clamped short-circuit protection of IGBT's," *IEEE Trans. Ind. Appl.*, vol. 35, no. 2, pp. 477–486, Mar./Apr. 1999.

[30] R. Hermann, S. Bernet, Y. Suh, and P. Steimer, "Parallel connection of Integrated Gate Commutated Thyristors (IGCTs) and diodes," *IEEE Trans. Power Electron.*, vol. 24, no. 9, pp. 2159–2170, Sept. 2009.

[31] H. Bai, Z. Zhao, M. Eltawil, and L. Yuan, "Optimization design of high-voltage-balancing circuit based on the functional model of IGCT," *IEEE Trans. Ind. Electron.*, vol. 54, no. 6, pp. 3012–3021, Dec. 2007.

[32] P. Palmer, H. Rajamani, and N. Dutton, "Experimental comparison of methods of employing IGBTs connected in series," *Electric Power Applications, IEE Proceedings* -, vol. 151, no. 5, pp. 576–582, Sept. 2004.

[33] A. Morozumi, K. Yamada, T. Miyasaka, S. Sumi, and Y. Seki, "Reliability of power cycling for IGBT power semiconductor modules," *IEEE Trans. Ind. Appl.*, vol. 39, no. 3, pp. 665–671, May/June 2003.

[34] S. Gekenidis, E. Ramezani, and H. Zeller, "Explosion tests on IGBT high voltage modules," in *Power Semiconductor Devices and ICs, 1999. ISPSD '99. Proceedings., The 11th International Symposium on*, 1999, pp. 129–132.

[35] M. Rahimo, U. Schlapbach, A. Kopta, R. Schnell, and S. Linder, "SPT$^+$, the next generation of low-loss HV-IGBTs," in *Proceedings of PCIM Europe 2005*, Nuremberg, Germany, June 2005.

[36] "5SMY 12N4500 IGBT-Die data sheet," ABB Switzerland Ltd Semiconductors, Lenzburg, Switzerland.

[37] M. Rahimo, A. Kopta, U. Schlapbach, J. Vobecky, R. Schnell, and S. Klaka, "The Bi-mode Insulated Gate Transistor (BIGT) a potential technology for higher power applications," in *Power Semiconductor Devices IC's, 2009. ISPSD 2009. 21st International Symposium on*, June 2009, pp. 283–286.

[38] Y. Haraguchi, S. Honda, K. Nakata, A. Narazaki, and Y. Terasaki, "600V LPT-CSTBT$^{\mathrm{TM}}$ on advanced thin wafer technology," in *Power Semiconductor Devices and ICs (ISPSD), 2011 IEEE 23rd International Symposium on*, May 2011, pp. 68–71.

[39] A. Kopta, M. Rahimo, U. Schlapbach, R. Schnell, and D. Schneider, "High voltage SPT$^+$ HiPak modules rated at 4500V," in *Proceedings of PCIM Europe 2007*, Nuernberg, Germany, 2007.

[40] T. Wikstrom, T. Stiasny, M. Rahimo, D. Cottet, and P. Streit, "The corrugated p-base IGCT – a new benchmark for large area SQA scaling," in *Power Semiconductor Devices and IC's, 2007. ISPSD '07. 19th International Symposium on*, May 2007, pp. 29–32.

[41] M. Bragard, M. Conrad, H. van Hoek, and R. De Doncker, "The Integrated Emitter Turn-Off Thyristor (IETO) – An innovative thyristor-based high power semiconductor device using MOS assisted turn-off," *IEEE Trans. Ind. Appl.*, vol. 47, no. 5, pp. 2175–2182, Sept.-Oct. 2011.

[42] T. Butschen, G. Etxeberria, H. Stagge, and R. De Doncker, "Gate drive unit for a Dual-GCT," in *Power Electronics and ECCE Asia (ICPE ECCE), 2011 IEEE 8th International Conference on*, June 2011, pp. 2419–2426.

[43] S. Tschirley and S. Bernet, "Automated testing of high power semiconductor devices," in *Proc. PELINCEC 2005*, Warsaw, Poland, 2005.

Felipe Filsecker was born in Viña del Mar, Chile, in 1983. He received his degree in Electrical Engineering from the Pontificia Universidad Católica de Valparaíso, Valparaíso, Chile, in 2009. He is now working towards the Ph.D. degree at the Technische Universität Dresden, Dresden, Germany. His research topics include medium voltage converters and power semiconductors. In 2009 he obtained the Second Prize Paper Award from the Power Electronic Devices and Components Committee.

Rodrigo Alvarez was born in Santiago, Chile, in 1981. He received the M.Sc. degree in Power Electronics at the Universidad Técnica Federico Santa María, Valparaíso, Chile in 2006 and the Ph.D. degree at the Technische Universität Dresden, Dresden, Germany in 2012, where he continues working as a research assistant. He has published papers in the areas of medium voltage converters and application of power semiconductors. In 2009 he obtained the Second Prize Paper Award from the Power Electronic Devices and Components Committee.

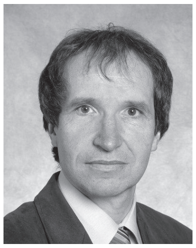

Steffen Bernet (M'97) received the Diploma degree in electrical engineering from Dresden University of Technology, Dresden, Germany, in 1990 and the Ph.D. degree in electrical engineering from Ilmenau University of Technology, Ilmenau, Germany, in 1995.

During 1995-1996, he had a Postdoctoral position with the Department of Electrical and Computer Engineering, University of Wisconsin, Madison. In 1996, he joined ABB Corporate Research, Heidelberg, Germany, where he led the Electrical Drive Systems Group and, from 1999 to 2000, was a Subprogram Manager responsible for the ABB research in the areas of power-electronics systems, drives and electric machines. From 2001 to 2007, he was a Professor of power electronics in Berlin University of Technology, Berlin, Germany. Since June 2007, he has been a Professor in Dresden University of Technology. During the past 17 years, he has conducted comprehensive research on power semiconductors, static power converters, and ac motor drives. He has published more than 90 papers in the field of power electronics.

Dr. Bernet is the recipient of the 2005 Second Prize Paper Award of the IEEE Power Electronics Specialists Conference and the IEEE Industry Applications Society Committee Second Prize Paper Awards from the Industrial Power Converter Committee and the Power Electronic Devices and Components Committee.